# Temperature Dependence of One-Component Permeation through a Silicalite-1 Membrane

**Wridzer J. W. Bakker, Leo J. P. van den Broeke, Freek Kapteijn, and Jacob A. Moulijn**
Dept. of Chemical Engineering, CPT-STM, Delft University of Technology,
Julianalaan 136, 2628 BL Delft, The Netherlands

*The one-component steady-state permeation of gases through a silicalite-1 zeolite composite membrane as a function of the temperature is studied from 190 to 680 K for light hydrocarbons, noble gases, and some inorganic gases. In general, with increasing temperature the permeance shows a maximum followed by a minimum. For gases weakly adsorbed the permeance has only a minimum and for gases strongly adsorbed only a maximum is observed in the permeance. The permeance for various gases, for a feed pressure of 101 kPa, span four orders of magnitude. The lowest permeation is for i-butane at 300 K: a permeance of* $0.07 \times 10^{-8}$ $mol \cdot m^{-2} \cdot s^{-1} \cdot Pa^{-1}$. *The highest value is observed for methane: a permeance of* $70 \times 10^{-8}$ $mol \cdot m^{-2} \cdot s^{-1} \cdot Pa^{-1}$ *at about 240 K. A comparison between the isobars and the temperature dependence of the steady-state permeance, both at 101 kPa, shows that at the temperature where the amount adsorbed vanishes the permeance starts to increase. The temperature dependence of the steady-state fluxes through the silicalite-1 membrane can be described only if two diffusion mechanisms are taken into account. For high occupancies the mass transport can be described by equilibrium adsorption followed by surface diffusion and for low occupancies the mass transport can be described by activated gaseous diffusion. With increasing temperature the mass-transport mechanism shifts from the surface diffusion regime to the activated gaseous diffusion regime. With these two diffusivities modeling results agree well with experimental results for the one-component flux through the silicalite-1 zeolite membrane.*

## Introduction

Diffusion in microporous materials is studied from both a fundamental and a practical point of view. Because of the well-defined pore structure of zeolites, the mass transport in these materials is extensively studied. The use of microporous materials in various catalytic and separation processes is another point of investigation. For a zeolite membrane it will be possible to combine catalytic activity and separation. In this work the temperature dependence of the one-component permeation through a silicalite-1 zeolite membrane has been studied.

Results are reported for the one-component steady-state permeation of 15 different gases through a silicalite-1 composite membrane as function of the temperature over the range of 190 to 680 K. The gases can be divided into the following three groups, the noble gases (He, Ne, Ar, Kr, and Xe), inorganic molecules ($H_2$, $N_2$, CO, $CO_2$, and $SF_6$), and light hydrocarbons ($CH_4$, $C_2H_6$, $C_3H_8$, $n$-$C_4H_{10}$, and $i$-$C_4H_{10}$). Also, results are presented for the equilibrium amount adsorbed on silicalite-1 as a function of the temperature; isobars at 101 kPa over the temperature range of 200 to 600 K. From these isobars the entropy and the enthalpy of adsorption are determined using the Langmuir isotherm. The presented results for the permeance, as a function of the temperature, clearly demonstrate the existence of two different mass-transport regimes in the silicalite-1 crystals.

Generally, the following behavior for the permeation as a function of the temperature is observed. Initially, the permeation increases with increasing temperature and goes through a maximum and then decreases. By further increasing the temperature the permeation reaches a minimum and in-

---

Correspondence concerning this article should be addressed to L. J. P. van den Broeke.

Present address of W. J. W. Bakker: Akzo Nobel Central Research, Dept. RTA, P.O. Box 9300, 6800 SB Arhnem, The Netherlands.

creases again. At low temperatures adsorption dominates and the permeation behavior can be described by adsorption followed by surface diffusion. The maximum in the permeation can be explained in terms of activated diffusion of adsorbed molecules. The surface diffusivity increases with temperature, and the amount adsorbed decreases with temperature. A comparison of the permeation and the isobar shows that the minimum in the permeation occurs at the temperature where the amount adsorbed in the silicalite-1 vanishes. The fact that the flux increases again at high temperatures can be explained with the so-called gas translation diffusion (Xiao and Wei, 1992a). At high temperatures there is a relatively small amount of the molecules in the adsorbed phase. For this situation the kinetic energy of the molecules in the zeolite pore dominates, and the molecules retain their gaseous character. But the molecules still have to overcome an energy barrier by passing from the channels to intersections, and vice versa. This is also an activated diffusion process. For normal Knudsen diffusion it is not possible to have an increase in the flux with an increase in the temperature.

This possibility of two different diffusion regimes in zeolites has recently been discussed by Xiao and Wei (1992a). The existence of two different diffusion regimes is in agreement with the mass transport of gases in other inorganic membranes, like glass membranes. See, for example, Hwang and Kammermeyer (1966), Shindo et al. (1983a), and Shelekin et al. (1995).

### *Micropore diffusion theory*

Diffusion in microporous media is described in terms of adsorption and surface diffusion; mass transport takes place in an adsorbed phase and can be pictured as molecules hopping between fixed sites. For the mass transport an activation energy of diffusion has to overcome (Barrer, 1941; Barrer and Jost, 1949; Reed and Ehrlich, 1981; Van den Broeke, 1995). This model for micropore diffusion has been extended by Xiao and Wei (1992a). Diffusion in zeolites is described as an activated process, and different situations are discussed in terms of different diffusional paths. In this way the hopping model, called the solid vibration model, has been derived, and an activated gas-phase diffusion model, called the gas translation model, is obtained. A different derivation of an activated gaseous diffusion coefficient for micropore diffusion has been given by Petropoulos and Hadvredaki (1986).

It is generally accepted that the concentration dependence of the Fick micropore or surface diffusivity is given by the Darken equation, $D_F = D_S(0)\,(d\ln P/d\ln q)$ (Chen and Yang, 1991; Kärger and Ruthven, 1992; Krishna, 1993; Van den Broeke, 1995). This relation relates the Fick diffusivity to an intrinsic diffusivity $D_S(0)$. The thermodynamic factor, $\Gamma = d\ln P/d\ln q$, relates the gas-phase pressure to the amount adsorbed and is obtained when the gradient in the chemical potential is used as the driving force for diffusion. Using the concept of transition-state theory, Chen and Yang (1991) derived a modified form of the Darken relation that takes into account the effect of the constriction of the zeolite structure on the mass transport. With this model different behaviors for the one-component Fick diffusivity in different zeolites, as a function of the amount adsorbed, are described. It has been found that one-component diffusion in MFI zeolites (silicalite-1 and ZSM-5) is a strong function of the amount adsorbed. The diffusion of hydrocarbons, including 2-methylbutane and benzene, in ZSM-5 has been studied by Xiao and Wei (1992b). For a loading higher than four molecules per unit cell, the Fick diffusivity increases with an increase in the amount adsorbed. This behavior is confirmed by Molecular Dynamics simulations for one-component diffusion of methane in silicalite-1 (Maginn et al., 1993).

### *Microporous membranes*

*Zeolite Membranes.* The results reported in this work were obtained with the same experimental setup and membrane synthesis procedure as described by Bakker et al. (1993) and by Geus et al. (1993). The permeation of one- and two-component gaseous systems through a silicalite-1 zeolite layer on a metal support, using a Wicke-Kallenbach diffusion cell, have been described by Bakker et al. (1993, 1996). Typical permeation behavior is demonstrated by the system composed of hydrogen, *n*-butane, and the silicalite-1 membrane. The steady-state selectivity for a 1:1 mixture of hydrogen and *n*-butane, for a feed pressure of 101 kPa, depends on the temperature. At room temperature the *n*-butane is adsorbed much stronger than the hydrogen, resulting in a separation factor of about 50, toward butane. With increasing temperature the amount adsorbed decreases, and the difference in mobility in the micropores will be the governing mechanism for separation. For this mechanism the membrane selectivity is in favor of the hydrogen. At 600 K a separation factor of about 4 toward hydrogen is found. Also, transient experiments have been performed at room temperature. In this type of experiment the approach to equilibrium is followed. For the permeation as a function of time, the faster moving but weakly adsorbed hydrogen shows a maximum in the permeation flux. The hydrogen enters the silicalite crystal first, because of its higher mobility, and is then replaced by the slower moving but stronger adsorbed butane. At steady state the binary flux of *n*-butane is higher than the hydrogen flux (Bakker et al., 1996; Van de Graaf et al., 1997).

Vroon et al. (1996) studied the synthesis of a silicalite-1 membrane on a ceramic support. Results are presented for the one-component permeation of methane, ethane, propane, *n*-butane, *i*-butane, and the permeation of some binary mixtures, as function of the partial pressure and temperature. The permeation of a 50-kPa methane and 50-kPa *n*-butane mixture, as a function of temperature clearly shows the effect of the stronger adsorbed *n*-butane on the weaker adsorbed methane. At a temperature of 373 K the flux of methane in the mixture has dropped by an order of magnitude as compared to the one-component situation.

Yan et al. (1995a, 1995b) presented results for a ZSM-5 membrane on an alumina support. Several synthesis experiments are described, which have been performed to find the optimal conditions to form a continuous zeolite layer. It was found that the one-component *n*-butane permeation was between 18 and 31 times higher than the *i*-butane permeation, over the temperature range of 303 to 458 K.

The group of Falconer and Noble (Bai et al., 1995; Baertsch et al., 1996) use a tube covered with silicalite-1 zeolite to study one- and two-component diffusion. Results are reported for the one-component permeation of five gases—hydrogen, argon, *n*-butane, *i*-butane, and sulfur hexafluoride—over the temperature range of 300 to 600 K. For hydrogen and argon a small minimum is observed in the permeance, as a function of the temperature. For the other three gases—$n$-butane, $i$-butane, and sulfur hexafluoride—the permeance increases monotonously with increasing temperature. At a temperature of 298 K the permeance of $n$-butane is higher than the permeance of $i$-butane; above this temperature $i$-butane permeates faster than $n$-butane (Bai et al., 1995). Results are also reported for aromatic hydrocarbon vapors permeating through the silicalite-1 membrane. Over the temperature range of 380 to 480 K it was found that the one-component permeance of the three xylene isomers, benzene, ethylbenzene, and toluene all increase with an increase in temperature. The sequence of the permeance did not follow the sequence of the kinetic diameter. For various binary mixtures of the aromatic hydrocarbons it was observed that the faster permeating species were slowed down to the rate of the slower permeating molecules, and as a consequence no separation is possible (Baertsch et al., 1996).

Nishiyama et al. (1996) reported results of one-component permeation through a Ferrierite zeolite membrane over the temperature range of 295 to 385 K. For a number of gases, including hydrogen, methane, oxygen, and carbon dioxide, a minimum is observed in the one-component permeation as a function of the temperature.

*Carbon Molecular Sieve Membranes.* Membranes of microporous activated carbon have been used by Barrer and coworkers (Ash et al., 1967, 1968) to study the diffusion in porous materials. Koresh and Soffer (1980) used fibrous carbon molecular sieves (CMS) and carbon molecular sieve membranes (Koresh and Soffer, 1983, 1986) to study the effect of pore structure and pore opening on mass transport. By gradually enlarging the pore openings of the carbon from 0.31 nm to 0.56 nm the cross section related to adsorption and diffusion of various molecules was established. Recently, with the development of carbon molecular sieves, interest in this type of microporous membrane has been renewed.

Chen and Yang (1994) developed a carbon molecular sieve membrane on a macroporous graphite support by controlled pyrolysis. A carbon molecular sieve layer of 15-$\mu$m thickness was obtained; the support thickness is 0.457 cm. Steady-state permeation experiments were performed for methane, ethane, and binary mixtures of these gases. From the concentration dependence of the single-component diffusivities the binary fluxes could be predicted using a loading ratio correlation for the isotherms.

Rao and Sircar (1993) developed a CMS membrane for the separation of hydrogen from small hydrocarbons. Results are reported for permeation of a mixture of hydrogen, methane, ethane and propane at 295 K. The mass transport through the micropores, with a diameter of about 1 nm, is by adsorption and surface diffusion. Separation was achieved by the difference in the amount adsorbed. Although the mobility of the hydrogen in the CMS membrane is higher than the mobility of the hydrocarbons, the membrane selectivity is in favor of the more strongly adsorbed hydrocarbons, rather than for the hydrogen that is relatively weakly adsorbed.

This behavior is completely analogous to the behavior of a mixture of hydrogen and $n$-butane through the silicalite-1 membrane, as studied by Bakker et al. (1996).

*Glass Membranes.* Kammermeyer and coworkers (Hwang and Kammermeyer, 1996; Hwang, 1968; Tock and Kammermeyer, 1969) and Inoue and coworkers (Shindo et al., 1983a, 1983b; Okubo and Inoue, 1989) studied the one-component diffusion in mesoporous Vycor glass membranes with a pore diameter of about 40 nm. Okubo and Inoue (1989) studied the permeation through a modified glass membrane, with a pore diameter of about 4 nm. The permeation results for this modified membrane show the same trend as was observed for the membrane with the larger pore diameter. In the modified glass membrane the permeation was one order of magnitude smaller as compared to the original glass membrane.

The various results for the adjusted permeance, $\Pi T^{1/2}$, of noble gases, nitrogen, and carbon dioxide as a function of the temperature (200–600 K) through glass membranes all show the same behavior. As the temperature is increased, starting at about 200 K, the adjusted permeability decreases, but for most of the gases it reaches a minimum around 300 K, and by further increasing the temperature the adjusted permeability starts to increase.

Ma and coworkers (Bhandarkar et al., 1992; Shelekhin et al., 1995) studied the permeation through a bidisperse microporous glass membrane, over the temperature range of 300 to 700 K. The result for the permeability of helium, methane, and carbon dioxide all increase with increasing temperature. The pore diameter of this glass membrane ranges from 0.5 nm to 1.5 nm.

The objective of this work is to present and interpret results for the temperature dependence of the flux of simple gases through a silicalite-1 membrane. The experimental results are described by a combined surface and activated gaseous diffusion model. Confirmed by the one-component permeation results for the silicalite-1 membrane, a general model for mass-transport micropores is available. For low temperatures the transport is by adsorption and surface diffusion, and for high temperatures mass transport is by activated gaseous diffusion. As a consequence of the fact that a second diffusion mechanism exists for zeolitic diffusion, helium, which is essentially nonadsorbing in silicalite-1, also has a significant flux through the zeolite crystals of the membrane, for elevated temperatures.

## Diffusion in Microporous Materials

Following Xiao and Wei (1992a) we start with the most general expression for the Fick diffusion coefficient

$$D_F = \frac{u\lambda}{z}\exp\left(-\frac{E_D}{RT}\right), \tag{1}$$

with $u$ the velocity of the diffusing molecules, $\lambda$ the diffusional free length, $z$ a constriction or probability factor, and $E_D$ the activation energy for diffusion.

For the silicalite-1 zeolite it will be shown that two different diffusion regimes are possible, depending on the temperature. For low temperatures diffusion takes place by diffusion in an adsorbed phase. If the temperature is increased, the amount adsorbed will decrease and above a given temperature no adsorbed phase will be present in the zeolite channels and the mass transport is by activated gaseous diffusion. The former will be denoted as surface diffusion, the latter as gas translation diffusion.

### Temperature dependence of the flux

We have extended the description of Xiao and Wei (1992a), and we assume that for a given temperature and loading both the surface diffusion and the activated gas translation diffusion contribute to the overall mass transport through the silicalite-1 membrane. For the total steady-state flux through the membrane we write

$$J_{tot} = J_S + J_{GT}, \tag{2}$$

with $J_S$ the flux given by the mass transport in silicalite-1, which takes place by surface diffusion, and $J_{GT}$ the flux given by the mass transport, which takes place by activated gas translation diffusion.

### Surface diffusion

For low temperatures an adsorbed phase is present in the zeolite pore. In this adsorbed phase the mass transport takes place by molecules jumping between adsorption sites. Assuming a random walk mechanism for mass transport, Eq. 1 gives the following relation for the surface diffusion coefficient

$$\begin{aligned} D_S(q) &= \frac{1}{z}\lambda^2 \nu(q) \exp\left(-\frac{E_{D,S}}{RT}\right) \\ &= D_S^0(q)\exp\left(-\frac{E_{D,S}}{RT}\right), \end{aligned} \tag{3}$$

where $\lambda$ is the distance between two adjacent sites, which is equal to the diffusional length. The velocity of the diffusing molecules is related to the jump frequency, $\nu$, of the adsorbed molecules by $u = \lambda \nu$. The flux through the silicalite-1 membrane for this situation is given by

$$J_S = \epsilon \rho D_S(q)\frac{dq}{dx}, \tag{4}$$

with $\epsilon$ the porosity of the support and $\rho$ the density of silicalite-1.

In general the surface diffusivity is a function of the amount adsorbed, $q$ (Chen and Yang, 1991). With the driving force for diffusion given by the gradient in the chemical potential, one can derive a relation between the Fick diffusivity and an intrinsic diffusivity (Krishna, 1993; Van den Broeke, 1995). The concentration dependence of the (Fick) surface diffusion in Eq. 3 is then given by

$$\begin{aligned} D_S(q) &= D_S^0(q)\exp\left(-\frac{E_{D,S}}{RT}\right) \\ &= D_S(0)\frac{d\ln P}{d\ln q} \\ &= D_S(0)\Gamma. \end{aligned} \tag{5}$$

This equation is also known as the Darken equation, and used to introduce some quantities. The diffusivity $D_S^0$ is generally referred to as a limiting diffusivity, which is independent of the temperature. The diffusivity $D_S(0)$ is referred to as an intrinsic diffusivity, which is independent of the amount adsorbed. The results to be presented below will be given in terms of $D_S^0(0)$. The thermodynamic correction factor $\Gamma$ can be calculated from the adsorption isotherm.

### Equilibrium adsorption

Often the Langmuir isotherm is used to describe the relation between the amount adsorbed, $q$, and the gas phase pressure, $P$,

$$\theta = \frac{q}{q_{\text{sat}}} = \frac{bP}{1+bP}. \tag{6}$$

The fractional surface occupancy $\theta$ is also a function of the temperature. The temperature dependence is given by the Langmuir parameter

$$\begin{aligned} b &= b^0 \exp\left(\frac{-\Delta H}{RT}\right) \\ &= \exp\left(\frac{\Delta S}{R} - \frac{\Delta H}{RT}\right). \end{aligned} \tag{7}$$

In this work we assume that the entropy of adsorption, $\Delta S$, and the enthalpy of adsorption, $-\Delta H$, are constant. For Langmuir adsorption the thermodynamic correction factor, see Eqs. 5 and 6, is given by

$$\begin{aligned} \Gamma &= \frac{q_{\text{sat}}}{q_{\text{sat}} - q} \\ &= \frac{1}{1-\theta} \end{aligned} \tag{8}$$

### Gas translation diffusion

For high enough temperatures no well-defined adsorbed phase will exist in the zeolite pore. Following Xiao and Wei (1992a), we say that the molecules inside the silicalite-1 pores retain their gaseous character, but for diffusion, from site-to-site, the molecules have to overcome an energy barrier imposed by the pore structure.

Again, the diffusivity can be derived from Eq. 1. The velocity of the diffusing molecules is obtained from the kinetic gas theory, where the diffusional length is denoted by $\lambda$.

$$D_{GT} = \frac{\lambda}{z}\sqrt{\frac{8RT}{\pi M}}\exp\left(-\frac{E_{D,GT}}{RT}\right). \tag{9}$$

For this situation the flux is given by

$$J_{GT} = \epsilon D_{GT}\frac{1}{RT}\frac{dP}{dx}. \tag{10}$$

The preceding theory, with the separate contributions is demonstrated in Figure 1 for the permeance of krypton. Also, plotted is the modified permeance, $\Pi T^{1/2}$, from which the

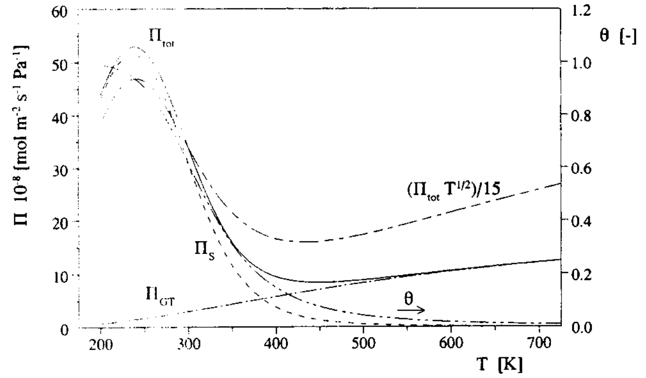

**Figure 1. Contribution of surface and gas translation diffusion to the total permeance Π, of krypton, and adjusted permeance Π $T^{1/2}$.**

temperature dependence is better observed. In this way the total temperature dependence of the activated gaseous flux is taken into account; see Eqs. 9 and 10.

### *Mass balance and permeance*

The flux through the silicalite-1 membrane is calculated from the mass balance over the membrane, at the steady state. In the mass balance the partial feed pressure, the permeate pressure, and the feed and the sweep gas flow rate are taken into account. As is shown below, upon heating the flux through the membrane changes with temperature. Therefore, the partial pressure difference over the membrane changes as the temperature changes. The permeance is used to compensate for the change in the partial pressure difference over the membrane. The permeance, Π, is related to the flux and the partial pressure difference over the membrane, $\Delta P$, in the following way

$$\Pi = \frac{J}{\Delta P}. \tag{11}$$

### *Simulations*

Combining Eqs. 2 to 10 the total flux through the zeolite membrane is given by

$$J_{\text{tot}}(T) = \epsilon \left[ \rho q_{\text{sat}} D_S^0(0) \frac{1}{1-\theta} \exp\left( -\frac{E_{D,S}}{RT} \right) \frac{d\theta}{dx} + \frac{\lambda}{z} \sqrt{\frac{8}{\pi MRT}} \exp\left( -\frac{E_{D,GT}}{RT} \right) \frac{dp}{dx} \right]. \tag{12}$$

It is noted that in this equation the occupancy $\theta$ is a function of the temperature, given by Eqs. 6 and 7.

In the paper of Xiao and Wei (1992a) a general picture is given of diffusion in MFI zeolite crystals; the activated gas translation diffusion was discussed in detail. For the zeolite structure studied in this work the activation energy for the gas translation diffusion can be interpreted as the difference in the potential energy, $U$, between a molecule in the intersections and in the channels. This can be written as

$$E_D = |U_{\max} - U_{\min}|. \tag{13}$$

The potential energy can be calculated from, for example, the 6-12 Lennard-Jones potential. The distance between the sites also determines the diffusional path, $\lambda$, for surface and gas translation diffusion; in silicalite-1 the distance between two adjacent sites is about 1 nm. An interesting behavior is seen for the intrinsic diffusivity as a function of the ratio of the kinetic diameter to the channel diameter (cf. figure 10 of the Xiao and Wei paper). If the ratio of the kinetic diameter to the channel diameter is smaller than 0.6, the diffusivity is more or less independent of this ratio. One can say that diffusion takes place in the Knudsen regime. On the other hand, if the kinetic diameter approaches the channel diameter, the diffusivity decreases sharply. This diffusion regime is referred to as configurational diffusion.

In this work the relative contributions of surface diffusion and gaseous diffusion are investigated. In the simulation presented we have four unknown parameters. From Eq. 3 we have used the limiting diffusivity, $D_S^0(0)$, and the activation energy, $E_{D,S}$, and from Eq. 9, the diffusional length, $\lambda$, and the activation energy, $E_{D,GT}$, as fitting parameters. The diffusional length $\lambda$ for gas translation diffusion has been fitted because its interpretation is not completely clear. The equilibrium parameters are obtained from independent measurements of the amount adsorbed as a function of the temperature; isobars at 101 kPa over the range of 200 to 600 K.

*Boundary Conditions.* In the experimental setup the silicalite-1 membrane is facing the feed flow, and the metal support the helium purge flow. Assuming equilibrium between the gas phase and the adsorbed phase, we have for the feed side the following condition:

$$\theta(x=0) = \theta^* = \frac{bP}{1+bP}. \tag{14}$$

Because the metal support layer is much thicker than the zeolite layer, the transport by molecular diffusion through the support must be taken into account. This means there will be a concentration difference, over the support, which cannot be ignored. The concentration difference can be calculated from the flux through the support $N$ and the concentration $C$ at the purge side

$$N_1 = D_{12} \frac{dC_1}{dx} \Big|_{\text{support}} + \upsilon C_1 \tag{15}$$

with $D_{12}$ the molecular diffusion, which is also a function of the temperature. The molecular diffusion coefficient is calculated from the relation given by Fuller (Fuller et al., 1966).

$$D_{1,\text{He}} = \alpha \frac{T^{1.75}}{P} \frac{(M_1^{-1} + M_{\text{He}}^{-1})^{1/2}}{(V_1^{1/3} + V_{\text{He}}^{1/3})^2}, \tag{16}$$

with $\alpha = 1.01 \times 10^{-5}\ \text{g}^{1/2} \cdot \text{m}^2 \cdot \text{s}^{-1} \cdot \text{N} \cdot \text{K}^{-7/4}\ \text{mol}^{7/6}$. For example, for methane with the molecular diffusion $D_{\text{CH}_4,\text{He}} = 5 \times 10^{-5}\ \text{m}^2 \cdot \text{s}^{-1}$ at 300 K, and the gas velocity in the porous support of about $\upsilon = 0.01\ \text{m} \cdot \text{s}^{-1}$, this gives rise to a partial pressure difference of about 10 kPa over the metal support

**Table 1. Ingredients Used in the Synthesis of Silicalite-1 Zeolite Membrane WTSS-1c**

| Chemicals | Relative Amount |
|---|---|
| $SiO_2$ (Aerosil 200) | 100 |
| TPA | 195 |
| $OH^-$ | 65 |
| $H_2O$ | 14,000 |
| Synthesis time | 12 h |
| Synthesis temperature | 465 K |

of 3-mm thickness. The ideal gas law is used to calculate the pressure, at the interface of the silicalite-1 layer and the metal support, from the concentration.

This pressure is used to calculate the driving force for permeation, which is given by the difference in occupancy and the difference in partial pressure over the silicalite-1 layer. The model is fitted to the experimental flux by optimizing the values for the two activation energies for diffusion, the value for the diffusivity $D_S^0(0)$, and the value for the diffusional length $\lambda$.

## Experimental Section

### *Synthesis of the silicalite-1 membrane*

A continuous silicalite-1 layer with a thickness of 50-60 $\mu$m was grown in a membrane module containing a two-layer porous stainless-steel support. The support is 3 mm thick and covered with a 50-150-$\mu$m smooth top layer of metal wool. The wires of this top layer are 10 to 50 $\mu$m apart. The top layer is supported by a coarse sintered layer with an average pore size of about 200 $\mu$m. A synthesis mixture was prepared by using silica (Aerosil 200, Degussa), tetrapropylammonium (TPAOH and TPABr), and water. The relative amounts used are given in Table 1. The synthesis mixture was aged for 6 h under stirring, after which a clear solution was obtained. The module with the smooth top layer of the support was filled with the synthesis mixture, while the other section was closed with a Teflon plug. During the synthesis both sides of the module were closed with flange connections using Teflon sealing rings. A typical synthesis is carried out at 465 K for 12 h. A continuous zeolite layer that covers both the porous and the solid part of the membrane module is then being formed. In this way only two materials are needed, the zeolite and stainless steel, and no extra sealing is required. After the synthesis the membrane was washed with water and ethanol and the flange connections were removed and replaced by two flanges with tubing for gas supply and removal. During the permeation experiments copper sealing rings were used between the flange with the silicalite-1 membrane and the two flanges with the gas tubes.

**Table 2. Characterization of the Silicalite-1 Zeolite Membrane and Experimental Conditions for Permeation Experiments**

| | | |
|---|---|---|
| Pore diameter silicalite-1 | $d_p$ [nm] | 0.55 |
| Density of silicalite-1 | $\rho$ [g·cm$^{-3}$] | 1.76 |
| Thickness of silicalite-1 layer | $\delta$ [$\mu$m] | 50-60 |
| Diameter of silicalite-1 membrane | $2R_m$ [mm] | 20 |
| Thickness of two-layer metal support | $\Delta$ [mm] | 3.0 |
| Porosity of metal-support layer | $\epsilon$ | 0.52 |
| Temperature range | $T$ [K] | 190-680 |
| Pressure | $P$ [kPa] | 101 |
| Feed flow | $\Phi_f$ [mL(NTP)·min$^{-1}$] | 100 |
| Purge flow (helium) | $\Phi_p$ [mL(NTP)·min$^{-1}$] | 200 |

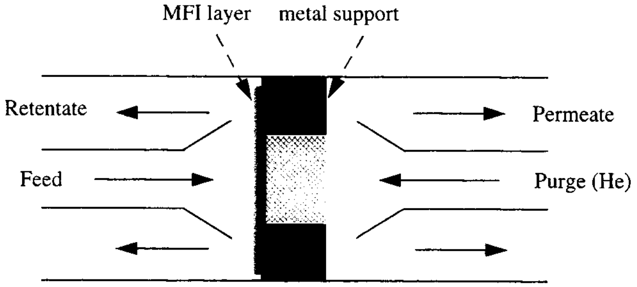

**Figure 2. Experimental setup: Wicke-Kallenbach cell.**

The characteristic parameters of silicalite-1 and the experimental setup are summarized in Table 2. The membrane module is schematically depicted in Figure 2. In this article permeation results are reported obtained from two metal supported silicalite-1 membranes that were prepared in an almost similar way. Table 3 indicates which membrane has been used for the permeation experiments.

*Calcination.* After the synthesis the template molecule tetrapropylammonium is present in the zeolite pores and no mass transport can occur through these pores. It is standard procedure to remove the template molecules by calcination. To test the quality of the membrane after the synthesis, neon was introduced at 100 kPa and 295 K at the feed side for 45 min, prior to calcination. Before calcination no neon signal was recorded by the mass spectrometer. During the calcination a 80/20 mixture of nitrogen and oxygen was flushed over both sides of the membrane. At one side of the membrane 20-kPa krypton was added to this mixture to observe the development of the permeation through the silicalite-1 layer. The calcination was started at room temperature, and a heating rate of 1 K·min$^{-1}$ to 673 K was used. The calcination was performed for 16 h, and the total pressure at both sides of the membrane was 100 kPa. Above 623 K the permeation

**Table 3. Intrinsic Diffusion Coefficients and Activation Energies for Diffusion***

| Gas | Membrane | $d_{kin}$** nm | $E_{D,S}$ kJ·mol$^{-1}$ | $D_S^0(0)$ $10^{-8}$m$^2$·s$^{-1}$ | $E_{D,GT}$ kJ·mol$^{-1}$ | $\lambda$ nm |
|---|---|---|---|---|---|---|
| He(/Ne) | WTSS-1c | 0.260 | 1.0 | 2.0 | 8.9 | 0.9 |
| Ne | WTSS-1c | 0.275 | 1.9 | 2.4 | 8.5 | 1.1 |
| Ar | WTSS-1c | 0.340 | 4.9 | 1.9 | 7.1 | 1.1 |
| Kr | WTSS-1c | 0.360 | 7.4 | 1.7 | 7.0 | 1.1 |
| Xe | WTSS-1c | 0.396 | 10.3 | 1.4 | 5.8 | 1.2 |
| $H_2$ | WTSS-1e | 0.289 | 2.1 | 1.5 | 8.3 | 0.9 |
| $N_2$ | WTSS-1e | 0.364 | 5.5 | 1.3 | 8.4 | 0.8 |
| CO | WTSS-1e | 0.376 | 7.1 | 0.9 | 9.9 | 0.8 |
| $CO_2$ | WTSS-1e | 0.330 | 9.6 | 0.7 | 10.3 | 0.9 |
| $SF_6$ | WTSS-1e | 0.550 | 17.4 | 0.8 | 12.4 | 0.8 |
| $CH_4$ | WTSS-1c | 0.380 | 8.8 | 3.9 | 7.9 | 1.0 |
| $C_2H_6$ | WTSS-1c | 0.390 | 10.5 | 1.7 | 7.2 | 1.0 |
| $C_3H_8$ | WTSS-1e | 0.430 | 12.2 | 0.75 | 11.4 | 0.9 |
| $n$-$C_4H_{10}$ | WTSS-1e | 0.430 | 13.7 | 0.40 | 13.1 | 0.8 |
| $i$-$C_4H_{10}$ | WTSS-1e | 0.500 | 15.1 | 0.15 | 13.5 | 0.8 |

* For all the gases the permeability was measured with helium as purge flow. The permeability for helium, from the purge to the feed side, was obtained from the permeation experiment with neon.

** From Breck (1974).

of krypton increased strongly with temperature, while at 673 K the permeation of krypton was constant, indicating that the zeolite pores were completely opened.

### *Experimental setup*

*Permeation Experiments.* The permeation measurements were performed according to the Wicke–Kallenbach method (Wicke and Kallenbach, 1941) with helium as purge flow. The feed, permeate, and retentate concentrations at both sides of the membrane were analyzed using a mass spectrometer. The pressure at the feed and the purge side can be varied independently between 0.1 and 1 MPa. The membrane module is placed with the zeolite membrane in a ventilation oven. During experiments the temperature was varied between 190 and 680 K. The temperature range of 190 to 298 K is obtained by cooling the oven with solid carbon dioxide (sublimation point of 194 K at 101 kPa).

The temperature-controlled permeation experiments are performed with a heating rate of 2 $K \cdot min^{-1}$. Before each experiment the oven was cooled to the desired temperature. During the cooling the flux through the silicalite-1 membrane was followed. If the flux was constant for about 30 min, steady state was assumed and the experiment was started by heating the oven. For all the temperature-controlled experiments, pure components were studied at atmospheric pressure. The feed flow rate, $\Phi_f$, was equal to 100 $mL \cdot min^{-1}$. The helium purge flow, $\Phi_p$, was equal to 200 $mL \cdot min^{-1}$. All the flows are in mL (NTP)/min. Prior to every experiment the oven with the membrane module was heated overnight to assure a clean membrane system. Typically, the oven was heated for 6 to 8 h at 538 K with a helium flow of at least 10 $mL \cdot min^{-1}$ at both sides of the membrane.

*Adsorption Experiments.* Adsorption experiments were performed with silicalite-1 crystals to obtain the isobars over the temperature range studied in this work. The isobars were obtained using a gravimetric technique. A conventional flow setup was used for this purpose; the change in the mass of the sample over the temperature range of 200 to 600 K was recorded. About 60 mg of silicalite-1 was put in a cup and exposed to a gas flow of 50 mL (NTP)$\cdot min^{-1}$, the heating rate was 1 $K \cdot min^{-1}$. The amount adsorbed on silicalite-1 as a function of the temperature was obtained, at a pressure of 101 kPa, by following the desorption from the crystals. The silicalite-1 crystals used to obtain the isobars were synthesized with the same recipe as was used in the membrane synthesis. Before the experiments the crystals were outgassed at 623 K and about 20 Pa for 6 to 8 h. The equilibrium results were corrected for flow and buoyancy effects.

## Results

### *Isobars*

To establish the diffusion regime where adsorption is important, the equilibrium amount adsorbed was obtained as a function of the temperature for most of the gases studied in this work. The results for a number of isobars over the temperature range of 200 to 600 K, at a pressure of 101 kPa, are given in Figure 3. The isobars for the first four *n*-alkanes have been reported previously by Bakker et al. (1996). The following sequence in the amount adsorbed is observed: $n\text{-}C_4H_{10} > C_3H_8 > C_2H_6 > CH_4$.

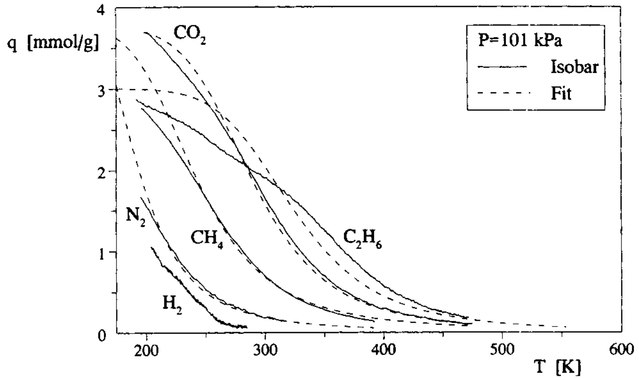

**Figure 3. Isobars on silicalite-1 crystals at 101 kPa over the temperature range of 200 to 600 K.**

Solid lines are experimental results, dashed lines are fits with the Langmuir model.

From Figure 3 it follows that by increasing the temperature, the amount adsorbed decreases, and above a given temperature, no measurable adsorption takes place. For the strongest adsorbed components, xenon, *i*-butane, and *n*-butane, this temperature is about 600 K. From the isobar at low temperatures it is clear that different components have a different saturation capacity, $q_{sat}$. Of the noble gases, neon and helium are essentially nonadsorbing; less than 0.1 $mmol \cdot g^{-1}$ of these gases is adsorbed at a temperature of 200 K.

The isobars are described with the Langmuir isotherm with the $b$ parameter as function of the temperature. The fits are obtained using (in Eq. 7) a constant enthalpy of adsorption and a constant entropy of adsorption. The results of these fits are given in Table 4. The saturation capacity of the different components has also been derived from the isobars. These results obtained from the isobars are used in the description of the temperature dependence of the one-component permeance.

### *Concentration dependent diffusion*

First we discuss the results for steady-state experiments as a function of the feed pressure to confirm the concentration

**Table 4. Equilibrium Adsorption Properties of Simple Gases in Silicalite-1, Obtained from Independent Isobaric Data**

| Gas | $M$ $g \cdot mol^{-1}$ | $\Delta S$ $J \cdot mol^{-1} \cdot K^{-1}$ | $-\Delta H$ $kJ \cdot mol^{-1}$ | $q_{sat}$ $mmol \cdot g^{-1}$ |
|---|---|---|---|---|
| He | 4 | 0 | 0.0 | 0.0 |
| Ne* | 20 | −37 | 5.0 | 5.2 |
| Ar | 40 | −49 | 13.2 | 5.1 |
| Kr | 84 | −57 | 19.3 | 4.9 |
| Xe | 131 | −69 | 29.9 | 3.1 |
| $H_2$ | 2 | −43 | 5.9 | 5.4 |
| $N_2$ | 28 | −50 | 13.8 | 5.4 |
| CO* | 28 | −55 | 17.9 | 5.1 |
| $CO_2$ | 44 | −58 | 24.1 | 5.0 |
| $SF_6^*$ | 146 | −74 | 37.9 | 2.1 |
| $CH_4$ | 16 | −70 | 22.6 | 4.5 |
| $C_2H_6$ | 30 | −74 | 30.4 | 3.0 |
| $C_3H_8^*$ | 44 | −80 | 38.2 | 2.4 |
| $n\text{-}C_4H_{10}$ | 58 | −85 | 45.9 | 2.2 |
| $i\text{-}C_4H_{10}$ | 58 | −82 | 34.1 | 1.5 |

* Data obtained from the fit for the flux.

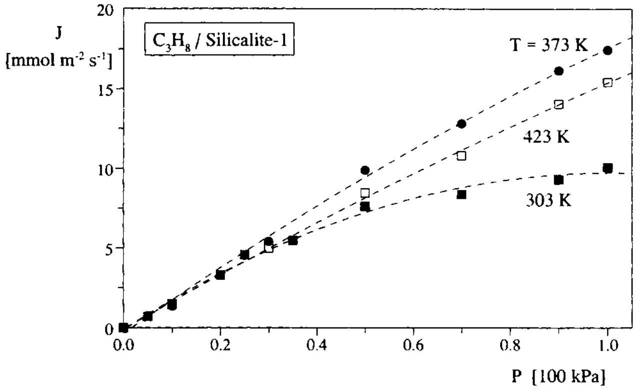

**Figure 4. One-component flux of propane through membrane WTSS-1e.**

Results are for three different temperatures, 303, 373 and 423 K, over the pressure range of 0 to 101 kPa. The dashed lines are a guide to the eye.

dependence of the one-component Fick diffusivity. In Figure 4 results are presented for propane as a function of the feed side pressure, for three different temperatures. At a temperature of 303 K the flux of propane shows a nonlinear dependence on the feed side (partial) pressure. At a higher temperature the amount adsorbed in the silicalite-1 crystals of the membrane is lower, and the flux shows a linear dependence on the feed side pressure. An interesting aspect is the fact that the propane flux at 373 K is higher than the flux at 423 K. The results presented in Figure 4 for propane indicate that the temperature dependence of the permeance will not follow an Arrhenius relation. It is therefore important to cover a large temperature range.

In Figure 5 the normalized surface diffusivity at 303 K is plotted as a function of the amount adsorbed. For the permeation of propane at 300 K the main contribution is by surface diffusion and we can neglect the contribution from the gas translation diffusion. The surface diffusivity is calculated from the total flux by using Eq. 4. As we will see below for the permeation of propane at 303 K, the gas translation contribution to the overall permeance is on the order of 1%. For ethane this is about 8%, at the same temperature. Clearly, the surface diffusivity varies with the amount adsorbed, and follows closely the thermodynamic factor, $\Gamma = 1/(1-\theta)^{-1}$. In the following the concentration-dependent surface diffusion is used in the description of the temperature dependence of the one-component permeance.

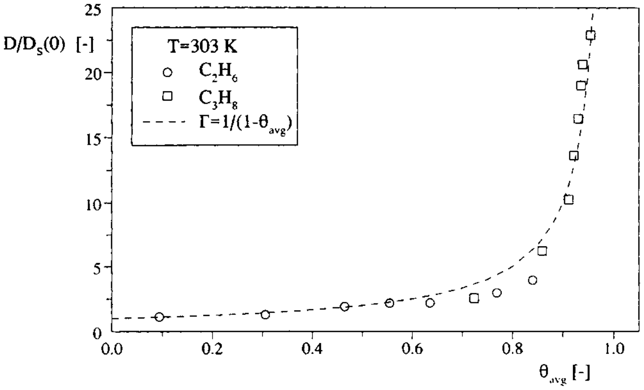

**Figure 5. Normalized one-component surface diffusivity for ethane and propane as function of the dimensionless amount adsorbed.**

Result obtained from the flux at a temperature of 303 K. The solid line is the thermodynamic factor obtained from the Langmuir isotherm, Eq. 9.

### *Permeance as a function of the temperature*

Figures 6 and 7 present the various results for the one-component permeation as a function of the temperature. Three different groups of gases are considered; noble gases, light hydrocarbons, and inorganic gases.

For the four linear alkanes, carbon monoxide, carbon dioxide, sulfur hexafluoride, krypton, and xenon a clear maximum and minimum is observed in the permeance through the silicalite-1 membrane. For helium (against neon), nitrogen, hydrogen, neon, and argon only a minimum in the permeance is seen. For *i*-butane the permeance increases continuously with increasing temperature.

All the results for the permeance are described with a concentration-dependent diffusion coefficient and taking the two different diffusion coefficients into account (see Eq. 12). The permeance is fitted with Eqs. 11 and 12, and the results of the fits were given earlier in Table 3. In Figure 7 the permeance of helium, from the purge to the feed side, is compared for three different feed gases.

### *One-component diffusion*

For the gases studied Figure 8 shows the corrected surface diffusion at a temperature of 303 K as function of the kinetic diameter. This is based on Eq. 5 and the data given earlier in Table 3, and taking the vanishing amount adsorbed in Eq. 8. We see that there are essentially two regions. In the first region the diffusivity is almost independent of the kinetic diameter. In the second region the diffusivity decreases rapidly with an increase in kinetic diameter. By going from argon to sulfur hexafluoride the diffusivity drops by a factor of 500.

A series of experiments have been performed with all 15 different gases at 673 K, with the same membrane (WTSS-1e). The results for the permeance are plotted in Figures 9a and 9b. In Figure 9a we have plotted the one-component permeance at a temperature of 673 K, as a function of the square root of the mass, and in Figure 9b as a function of the kinetic diameter. In both plots the same trend is seen—the permeance through the silicalite-1 layer decreases rapidly if the mass or the size of the permeating molecules increases. In Figure 9a we have also plotted the permeance, as a function of the square root of the mass, calculated with a constant activation energy of 10 kJ mol$^{-1}$ for the activated gaseous diffusion; this is the dashed line in Figure 9a.

## Discussion

### *Steady-state permeance as function of the temperature*

The following general behavior is observed for the permeance as a function of the temperature. Initially, the permeance goes through a maximum if the temperature is increased. If the temperature is further increased, a minimum is observed in the permeance.

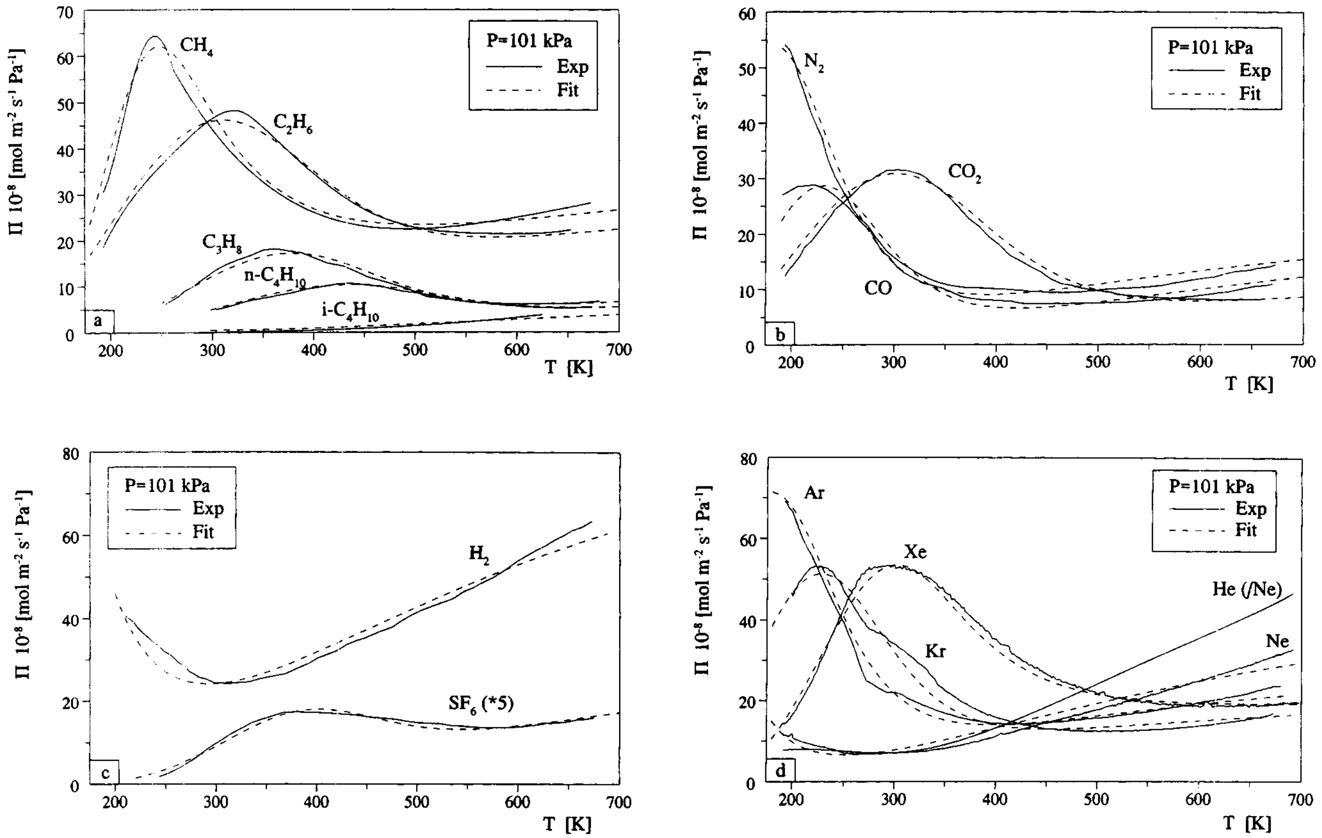

**Figure 6. One-component permeance at a pressure of 101 kPa as a function of the temperature (190 to 680 K).**

(*a*) Permeance of the hydrocarbons: $CH_4$ and $C_2H_6$ through membrane WTSS-1c, $C_3H_8$, $n-C_4H_{10}$, and $i$-$C_4H_{10}$ through membrane WTSS-1e. (*b*) Permeance of the inorganic gases: $N_2$, CO, and $CO_2$ through membrane WTSS-1e. (*c*) Permeance of the inorganic gases: $H_2$ and $SF_6$ through membrane WTSS-1e. (d) Permeance of the noble gases: He, Ne, Ar, Kr, and Xe through membrane WTSS-lc.

The maximum in the flux can be described by equilibrium adsorption and activated surface diffusion. For this case, mass transport takes place by molecules hopping between sites. This is an activated process and the diffusivity increases with temperature. The amount adsorbed is based on equilibrium and decreases with temperature. The sequence in the maxima of the permeance follows the sequence of the equilibrium amount adsorbed in silicalite-1. For the linear hydrocarbons this sequence is methane < ethane < propane < *n*-butane. The amount adsorbed is taken into account by the enthalpy of adsorption (see Table 4). The effect of the increase in the enthalpy of adsorption is that the amount adsorbed will increase, and therefore the maximum in the flux occurs at a higher temperature. The activation energy for dif-

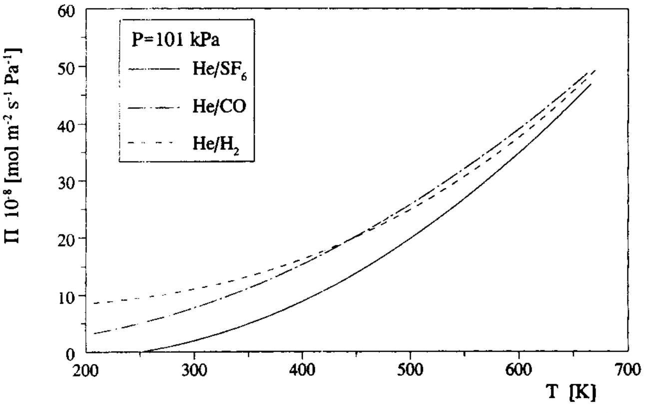

**Figure 7. Helium permeance through membrane WTSS-1e, from the purge to the feed side, as a function of the temperature for three different gases at the feed side.**

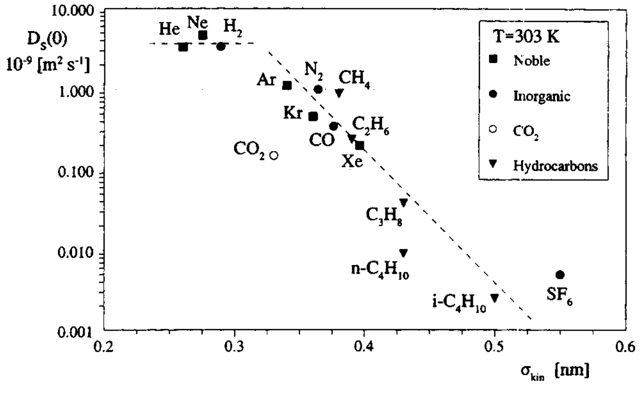

**Figure 8. One-component surface diffusion coefficient as a function of the kinetic diameter, at a temperature of 303 K.**

The dashed lines are a guide to the eye.

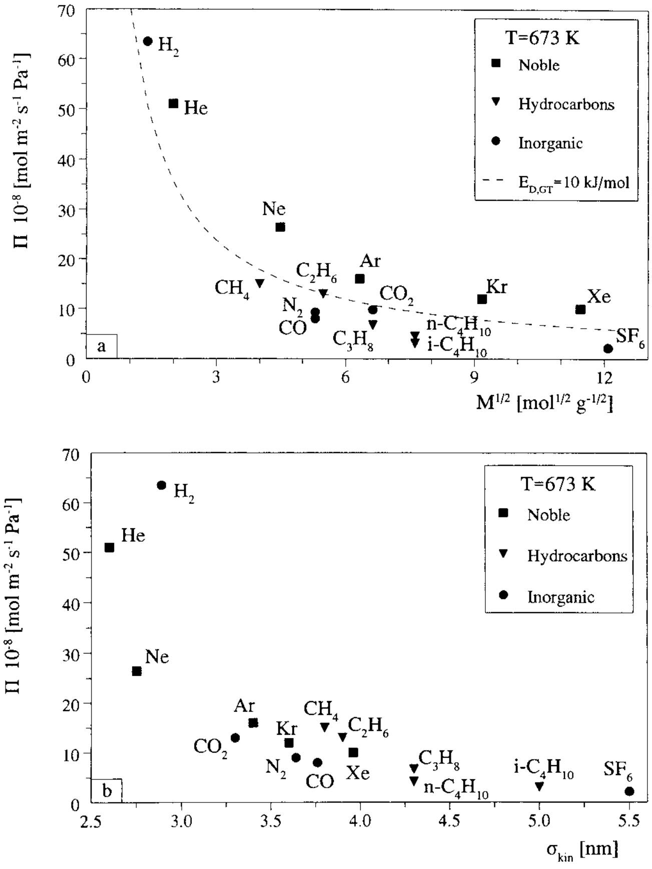

**Figure 9. One-component permeance for the different gases at 673 K.**

(a) As a function of the square root of the mass. (b) As a function of the kinetic diameter.

fusion has only an effect on the height of the maximum. One of the most interesting effects is the increase in the permeance if the temperature is further increased. This is clearly seen for methane and the noble gases.

For most of the gases studied the permeance increases with increasing temperature for a temperature above 650 K. For xenon and *n*-butane the permeance reaches a plateau between 650 and 673 K. The minimum in the flux occurs because, above a given temperature, the equilibrium amount adsorbed in the silicalite-1 pores vanishes. This increase in the permeance can only be described with a second diffusion mechanism. The explanation of the increasing trend is that an activated process must exist. This behavior is described with Eq. 9 for the gas translation diffusion coefficient. Without an additional term for the activation energy, Knudsen diffusion cannot describe the observed increase. It is noted that when adsorption increases, the minimum takes place at higher temperatures. From a comparison between the permeance and the isobars it is seen that the temperature of the minimum corresponds within 50 K with the temperature where the amount adsorbed vanishes.

*Permeation of i-Butane.* It seems that *i*-butane shows a different behavior as a function of the temperature when compared to the other gases; no maximum and no minimum is observed. This is because, for the permeation of *i*-butane, the contribution from surface diffusion is much smaller than the contribution from the gaseous diffusion. This becomes clear if the properties for *n*-butane and *i*-butane, as presented in Tables 3 and 4, are compared. From simulations it follows that if for *i*-butane, for example, the activation energy, $E_{D,S}$, was decreased to about 12 kJ$\cdot$mol$^{-1}$, a maximum and a minimum in the temperature dependence of the overall permeance would also be observed. So, the experimental and simulated results for *i*-butane confirm that a general theory for micropore diffusion is available.

*Counterdiffusion of Helium.* During the temperature programmed experiments, the helium flow from the purge to the feed side is recorded at fixed intervals (about every 30 K). The permeation of helium through the membrane depends on the amount of feed gas adsorbed (see Figure 7). Helium is hindered more by stronger adsorbed molecules; for helium to move through the gas phase, sufficient space is required inside the zeolite pores. This confirms that activated gas diffusion takes place in the zeolite pores.

At a temperature of 673 K, it is found that the helium permeates regardless of the kind of feed gas. For all the gases considered, permeance of the counterdiffusing helium lies around $50 \times 10^{-8}$ mol$\cdot$m$^{-2}\cdot$s$^{-1}\cdot$Pa$^{-1}$ at 673 K.

### *One-component diffusivities*

*Surface Diffusion.* From Figure 8 it follows that the surface diffusivity is almost constant for a kinetic diameter up to about 0.3 nm. This corresponds with a kinetic diameter to pore diameter ratio of 0.55. Above this ratio the corrected diffusivities decrease strongly, on the half logarithmic scale, with the kinetic diameter. A relatively large difference is observed for carbon dioxide; from an extrapolation based on the diffusivity of the other gases, the corrected diffusivity is about an order of magnitude lower than expected. We can say that at 300 K, for helium, neon, and hydrogen the diffusion is in the Knudsen regime; for the other gases, the diffusion is in the configurational regime.

*High Temperature Limit: Gas Translation Diffusion.* For a temperature above 650 K, almost no gas adsorption takes place in the silicalite-1 crystals. For this situation the mass transport will be solely determined by activated gaseous diffusion. From Figure 9 it follows that all the results for the permeance lie in a small band around an average activation energy for gas translation diffusion of about 10 kJ mol$^{-1}$. From the plot of the permeance as a function of the kinetic diameter, it follows, as expected, that the permeance strongly decreases with increasing size of the molecules.

From Table 3 it is clear that the diffusional length $\lambda$ is the same for all the gases. The distance of about 1 nm is clearly of intracrystalline dimensions, and is about the distance between two intersections.

### *Comparison with literature data*

*Permeation Through Zeolite Membranes.* For a number of different zeolite membranes permeation data have been reported in the literature. In Table 5 a comparison is made between other MFI membranes and a Ferrierite membrane. Ferrierite has a pore dimension similar to the MFI zeolites. Results are compared for the weakly adsorbed hydrogen, the moderately adsorbed methane, and the strongly adsorbed *n*-butane. Some differences are found from the permeation re-

**Table 5. Comparison of Reported One-Component Permeation Data through Different Zeolites Membranes***

| | | $\Pi\ 10^{-8}$ [$\mathrm{mol \cdot m^{-2} \cdot s^{-1} \cdot Pa^{-1}}$] | | | |
|---|---|---|---|---|---|
| Zeolite/Support | $\delta[\mu m]$ | $H_2$ | $CH_4$ | $n-C_4H_{10}$ | Reference |
| Ferrierite/alumina | — | 0.8 | 0.3 | — | Nishiyama et al. (1996) |
| ZSM-5/$\alpha$-$Al_2O_3$ | 10 | 1.0 | — | 1.11** | Yan et al. (1995b) |
| Silicalite-1/$\gamma$-alumina | 5 | 340 | — | 5.9 | Bai et al. (1995) |
| Silicalite-1/$\alpha$-$Al_2O_3$ | $<5$ | — | $10^{\dagger}$ | $3^{\dagger}$ | Vroon et al. (1996) |
| Silicalite-1/stainless steel | 50 | 15 | 30 | 5 | This work |

* Results are for pure component with a pressure of 101 kPa and a temperature of about 300 K; $\delta$ is the thickness of the zeolite membrane.
** At 381 K.
† Results obtained from flux, $\Pi = J/\Delta P$, with $\Delta P = 1 \times 10^5$ Pa.

sults through the various membranes. A number of explanations can be put forward. First of all, the membrane thickness has a distinct influence. Compared to the results presented in this work for a membrane with a thickness of $\delta = 50$ $\mu$m, the difference with Bai et al. (1995) for the permeation of hydrogen is on the order of a factor of 2, after a correction for the membrane thickness. The difference with Nishiyama et al. (1996) and Yan et al. (1995a) becomes larger after taking the membrane thickness into account. This may be caused by the fact that they also have a different type of zeolite layer and support. As discussed by Bakker et al. (1996) the mass-transport resistance of the metal support is much lower as compared to ceramic supports.

More interesting to compare is the observed trend for the permeation of, in particular, the hydrocarbons as a function of the temperature through the different MFI-supported membranes. For these gases a comparison is possible, with results presented by Vroon et al. (1996), by Bai et al. (1995), and by Yan et al. (1995a). The results presented by Vroon et al. (1996) for the flux of the first four *n*-alkanes and *i*-butane (cf. Figures 7 and 8), through a silicalite-1 layer on a $\alpha$-$Al_2O_3$ support, show a very similar behavior, as reported in this work. A maximum is observed in the flux of ethane, propane, and *n*-butane over the temperature range studied. For *i*-butane an increasing behavior is observed. It is noted that the authors just cited also find that, over the temperature range of 300 to 575 K, the flux of *n*-butane is always higher than the one obtained for *i*-butane. Yan et al. (1995a) reported results for a ZSM-5 layer on a $\alpha$-$Al_2O_3$ support, where *n*-butane permeates 18 to 31 times faster than *i*-butane over the temperature range of 303 to 458 K. On the other hand, Bai et al. (1995) reported results for the permeation of *n*-butane and *i*-butane through a silicalite-1 layer on a $\gamma$-alumina support that are different from the other results for MFI membranes. First of all no maximum is observed in the permeance of *n*-butane. Second, above 350 K, *i*-butane has always a higher permeance than *n*-butane (cf. Figure 3). Because all other groups find that the permeance of *n*-butane is higher than the *i*-butane permeance through MFI membranes, the result of Bai et al. (1995) is questionable.

## Conclusions

Results for the one-component steady-state gas permeation through a silicalite-1 zeolite membrane have been presented and modeled. Good agreement is obtained between the experimental and numerical results for the permeation through the silicalite-1 membrane. The permeation behavior can be described for a wide range of properties, including the enthalpy of adsorption, the activation energy for diffusion, and the size and the mass, of 15 different gases.

A new diffusion regime is established from the permeation through the silicalite-1 membrane. This regime is difficult to study with the conventional experimental techniques. It has been demonstrated that the temperature dependence of the steady-state fluxes, over the range of 190 to 680 K, can only be described if two diffusion mechanisms are taken into account. At conditions where a considerable amount is adsorbed, the diffusion takes place by mass transport in an adsorbed layer. This can be pictured as molecules jumping between adsorption sites. This is referred to as surface diffusion. For high temperatures, where virtually no adsorption takes place, the diffusion is described by gas transport diffusion. The existence of two different diffusion regimes is in agreement with the mass transport of gases in microporous glass membranes. Comparing the isobars for the equilibrium amount adsorbed on silicalite-1 at 101 kPa with the fluxes as function of the temperature, we see that the minimum in the fluxes occurs at the temperature where the amount adsorbed vanishes. At this temperature the one-component flux through the silicalite-1 membrane starts to increase. The diffusional path in the high-temperature range is about 1 nm. This is clearly an intracrystalline property and corresponds to the distance between two pore intersections.

## Acknowledgment

We gratefully acknowledge BNFL, UK, for support. Mr. M. J. G. Linders is thanked for performing most of the isobar experiments.

## Notation

$b^0$ = limiting value of the Langmuir adsorption parameter, $(100\ \mathrm{kPa})^{-1}$
$d_p$ = pore diameter, m
$M$ = molar mass, g $\mathrm{mol^{-1}}$
$R$ = gas constant, $\mathrm{J \cdot mol^{-1} \cdot K^{-1}}$
$R_m$ = diameter of zeolite membrane layer, m
$v$ = gas velocity, $\mathrm{m \cdot s^{-1}}$
$V$ = diffusional volume, $\mathrm{m^3}$
$x$ = space coordinate, m
$\alpha$ = constant in Fuller equation, $\mathrm{g^{1/2} \cdot m^2 \cdot s^{-1} \cdot N \cdot K^{-7/4} \cdot mol^{7/6}}$
$\Delta$ = thickness of support, m

### *Subscripts and superscripts*

avg = average amount adsorbed
$D$ = diffusion
$F$ = Fick diffusion
max, min = maximum, minimum in potential energy
sat = saturation capacity

## Literature Cited

Ash, R., R. W. Baker, and R. M. Barrer, "Sorption and Surface Flow in Graphitized Carbon Membranes: I. The Steady State," *Proc. R. Soc. A.*, **299,** 434 (1967).

Ash, R., R. W. Baker, and R. M. Barrer, "Sorption and Surface Flow in Graphitized Carbon Membranes: II. Time-Lag and Blind Pore Character," *Proc. R. Soc. A.*, **304,** 407 (1968).

Baertsch, C. D., H. H. Funke, J. L. Falconer, and R. D. Noble, "Permeation of Aromatic Hydrocarbon Vapors through Silicalite-Zeolite Membrane," *J. Phys. Chem.*, **100,** 7676 (1996).

Bai, C., M.-G., Jia, J. L. Falconer, and R. D. Noble, "Preparation and Separation Properties of Silicalite Composite Membranes," *J. Memb. Sci.*, **105,** 79 (1995).

Bakker, W. J. W., G. Zheng, F. Kapteijn, M. Makkee, J. A. Moulijn, E. R. Geus, and H. van Bekkum, "Single and Multi-component Transport Through Metal-supported MFI Zeolite Membranes," *Precision Process Technology*, M. P. C. Weijnen and A. A. H. Drinkenburg, eds., Kluwer, Dordrecht, The Netherlands, p. 425 (1993).

Bakker, W. J. W., F. Kapteijn, J. Poppe, and J. A. Moulijn, "Permeation Characteristics of a Metal-Supported Silicalite-1 Zeolite Membrane," *J. Memb. Sci.*, **117,** 57 (1996).

Barrer, R. M., "Migration in Crystal Lattices," *Trans. Farad. Soc.*, **37,** 590 (1941).

Barrer, R. M., and W. Jost, "A Note on Interstitial Diffusion," *Trans. Farad. Soc.*, **45,** 928 (1949).

Bhandarkar, M., A. B. Shelekin, A. G. Dixon, and Y. M. Ma, "Adsorption, Permeation, and Diffusion of Gases in Microporous Membranes: I. Adsorption of Gases on Microporous Glass Membranes," *J. Memb. Sci.*, **75,** 221 (1992).

Breck, D. W., *Zeolite Molecular Sieves*, Wiley, New York (1974).

Chen, Y. D., and R. T. Yang, "Concentration Dependence of Surface Diffusion and Zeolitic Diffusion," *AIChE J.*, **37,** 1579 (1991).

Chen, Y. D., and R. T. Yang, "Preparation of Carbon Molecular Sieve Membrane and Diffusion of Binary Mixtures in the Membrane," *Ind. Eng. Chem. Res.*, **33,** 3146 (1994).

Fuller, E. N., P. D. Schettler, and J. C. Giddings, "A New Method for Prediction of Gas-Phase Diffusion Coefficients," *Ind. Chem. Eng.*, **58,** 19 (1966).

Geus, E. R., H. van Bekkum, W. J. W. Bakker, and J. A. Moulijn, "High-Temperature Stainless Steel Supported Zeolite (MFI) Membranes: Preparation, Module Construction, and Permeation Experiments," *Microporous Mat.*, **1,** 131 (1993).

Hwang, S.-T., "Interaction Energy in Surface Diffusion," *AIChE J.*, **5,** 809 (1968).

Hwang, S.-T., and K. Kammermeyer, "Surface Diffusion in Microporous Media," *Can. J. Chem. Eng.*, **44,** 82 (1966).

Kärger, J., and D. M. Ruthven, *Diffusion in Zeolites*, Wiley, New York (1992).

Koresh, J. E., and A. Soffer, "Study of Molecular Sieve Carbons: 1. Pore Structure, Gradual Opening and Mechanism of Molecular Sieving," *J. Chem. Soc. Faraday Trans.*, **18,** 2457 (1980).

Koresh, J. E., and A. Soffer, "Molecular Sieve Carbon Permselective Membrane: 1. Presentation of a New Device for Gas Mixture Separation," *Sep. Sci.*, **18,** 723 (1983).

Koresh, J. E., and A. Soffer, "Mechanism of Permeation through Molecular-Sieve Carbon Membrane Part 1—The Effect of Adsorption and the Dependence on Pressure," *J. Chem. Soc. Farad. Trans. I*, **82,** 2057 (1986).

Krishna, R., "A Unified Approach to the Modelling of Intraparticle Diffusion in Adsorption Processes," *Gas Sep. Purif.*, **7,** 91 (1993).

Maginn, E. J., A. T. Bell, and D. N. Theodorou, "Transport Diffusivity of Methane in Silicalite from Equilibrium and Nonequilibrium Simulations," *J. Phys. Chem.*, **97,** 4173 (1993).

Nishiyama, N., M. Matsukata, and K. Ueyama, "Gas Permeation of Zeolite-Aluminum Composite Membranes," *Proc. World Congress of Chemical Engineering*, Vol. IV, San Diego, p. 834 (July 14–18, 1996).

Okubo, T., and H. Inoue, "Single Gas Permeation Through Porous Glass Modified with Tetraethoxysilane," *AIChE J.*, **35,** 845 (1989).

Petropoulos, J. H., and V. I. Havredaki, "On the Fundamental Concepts Underlying Henry-Law Adsorption and Adsorbed Gas Transport in Porous Solids," *J. Chem. Soc. Faraday Trans. I*, **82,** 2531 (1986).

Rao, M. B., and S. Sircar, "Nanoporous Carbon Membrane for Gas Separation," *Gas Sep. Purif.*, **7,** 279 (1993).

Reed, D. A., and G. Ehrlich, "Surface Diffusion, Atomic Jump Rates and Thermodynamics," *Surface Sci.*, **102,** 588 (1981).

Shelekhin, A. B., A. G. Dixon, and Y. M. Ma, "Theory of Gas Diffusion and Permeation in Inorganic Molecular-Sieve Membranes," *AIChE J.*, **41,** 58 (1995).

Shindo, Y., T. Hakuta, H. Yoshitome, and H. Inoue, "Gas Diffusion in Microporous Media in Knudsen's Regime," *J. Chem. Eng. Japan*, **16,** 120 (1983a).

Shindo, Y., T. Hakuta, H. Yoshitome, and H. Inoue, "A Dimensional Equation for Gas Diffusion in Microporous Media in Knudsen's Regime," *J. Chem. Eng. Japan*, **16,** 521 (1983b).

Tock, R. W., and K. Kammermeyer, "Temperature-Separation Factor Relationship in Gaseous Diffusion," *AIChE J.*, **15,** 715 (1969).

Van den Broeke, L. J. P., "Simulation of Diffusion in Zeolitic Structures," *AIChE J.*, **41,** 2399 (1995).

Van de Graaf, J. M., F. Kapteijn, and J. A. Moulijn, "Zeolitic Membranes," *Structured Catalysts and Reactors*, Chap. 19, A. Cybulski and J. A. Moulijn, eds., Marcel Dekker, New York, in press (1997).

Vroon, Z. A. E. P., K. Keizer, M. J. Gilde, H. Verweij, and A. J. Burggraaf, "Transport Properties of Alkanes through a Ceramic Thin Zeolite MFI Membrane, *J. Memb. Sci.*, **113,** 293 (1996).

Wicke, E., and R. Kallenbach, "Die Oberflächendiffusion von Kohlendioxyd in aktiven Kohlen," *Kolloid Z.*, **97,** 135 (1941).

Xiao, J., and J. Wei, "Diffusion Mechanism of Hydrocarbons in Zeolites: I. Theory," *Chem. Eng. Sci.*, **47,** 1123 (1992a).

Xiao, J., and J. Wei, "Diffusion Mechanism of Hydrocarbons in Zeolites: II. Analysis of Experimental Observations," *Chem. Eng. Sci.*, **47,** 1142 (1992b).

Yan, Y., M. Tsapatsis, G. R. Gavalas, and M. E. Davis, "Zeolite ZSM-5 Membrane Grown on Porous $\alpha$-$Al_2O_3$," *J. Chem. Soc., Chem. Commun.*, 227 (1995a).

Yan, Y., M. E. Davis, and G. R. Gavalas, "Preparation of Zeolite ZSM-5 Membrane by *In-Situ* Crystallization on Porous $\alpha$-$Al_2O_3$," *Ind. Eng. Chem. Res.*, **34,** 1652 (1995b).

*Manuscript received Dec. 26, 1996, and revision received May 1, 1997.*